Stochastic resonance in noise-induced transitions between self-oscillations and equilibria in spin-valve nanomagnets

M. d'Aquino,[1] C. Serpico,[2] R. Bonin,[3] G. Bertotti,[4] and I. D. Mayergoyz[5]
[1]*Dipartimento per le Tecnologie, Università degli Studi di Napoli "Parthenope", I-80143 Napoli, Italy*
[2]*Dipartimento di Ingegneria Elettrica, Università di Napoli "Federico II", I-80125 Napoli, Italy*
[3]*CSPP-LIM, Politecnico di Torino, Sede di Verrès, I-11029 Aosta, Italy*
[4]*Istituto Nazionale di Ricerca Metrologica (INRiM), I-10135 Torino, Italy*
[5]*ECE Department and UMIACS, University of Maryland, College Park, Maryland 20742, USA*
(Received 3 August 2011; revised manuscript received 21 November 2011; published 8 December 2011)

The thermally induced synchronization between magnetization transitions and "weak" ac excitations is studied for spin-transfer oscillators. A theoretical approach, based on the separation of time scales, is developed to investigate this physical phenomenon. By applying the appropriate averaging technique to the Fokker-Planck equation associated with the stochastic magnetization dynamics, a stochastic differential equation for the "slow" (energy) variable is derived. This equation is used to analyze intrawell thermal transitions between magnetization equilibria and self-oscillations. It is demonstrated that the thermally induced synchronization between magnetization transitions and ac excitation can be viewed as a stochastic resonance effect. It is shown that this effect occurs in spin-transfer nano-oscillators both in the classical case of subthreshold ac excitation as well as in the suprathreshold case. The theoretical predictions are in very good agreement with simulations of the Landau-Lifshitz-Slonczewski dynamics.

DOI: 10.1103/PhysRevB.84.214415 PACS number(s): 85.75.−d, 05.45.Xt, 05.10.Gg

I. INTRODUCTION

It is known that the interaction between injected spin-polarized currents and magnetization in multilayer magnetic nanosystems may excite large magnetization precessions far from equilibrium.[1] These spin-transfer-driven magnetization oscillations could be used in the design of current-controlled microwave oscillators integrable with semiconductor electronics.[2] It is believed that this type of spin-transfer nano-oscillators (STNOs) have great potential for advanced wireless applications. Typical STNOs have a spin-valve-like structure composed of a ferromagnetic layer, the magnetization of which is pinned to a given orientation (referred to as fixed layer), a nonmagnetic conducting spacer, and a thin ferromagnetic layer (referred to as free layer) where the magnetization dynamics takes place (see Fig. 1). Experimental[2] as well as theoretical studies[3] have revealed that magnetization dynamics in the presence of injected dc spin-polarized current admits two different regimes: equilibria or self-oscillations. Since STNOs have nanoscale dimensions, thermal fluctuations may induce transitions between different dynamical regimes, as shown by experimental observations[4–6] and theoretical studies.[7] When STNOs are subject to time-varying excitations (ac currents or external fields), the dynamical picture of magnetization dynamics may become very complex due to the possible onset of nonlinear resonance, quasiperiodicity, synchronization, and chaos.[8] Recently, the synchronization between multiple STNOs (Refs. 9 and 10) or synchronization with an external reference signal (often referred to as injection locking[11–19]) have been the focus of considerable research and interest.

In this paper, we consider an essentially different physical synchronization mechanism, namely, the synchronization of thermally induced transitions between different magnetization regimes (equilibria, self-oscillations) with "weak" external ac excitations (for instance, ac spin-polarized injected currents). In the absence of ac excitation, the STNO output signal exhibits random transitions between oscillating and stationary regimes. The transition rates increase monotonically with the temperature and are moderately low in typical experimental situations for nanoscale devices (in the range of kHz–MHz), whereas the frequency of magnetization self-oscillations lies in the GHz range.[2] We show that, when a weak ac current with frequency about one half of the transition rates is injected, synchronization between the aforementioned thermal transitions and the external signal may occur. This leads to the appearance of a strong periodic response of the system at the frequency of the external signal. We find that the amplitude of the response at the forcing frequency exhibits a nonmonotonic dependence on temperature, which is the generic signature of stochastic resonance.[20]

It is worthwhile to mention that stochastic resonance in STNOs has been the focus of recent experimental[21] and numerical[22] studies. The phenomenon of stochastic resonance has mostly been studied in connection with thermal transitions in multistable systems characterized by multiple stable fixed points. In such systems, the basic mechanism is usually understood by using the symmetric bistable double-well potential.[20] Although it is clear that the stochastic resonance phenomena may occur also in presence of multiple attractors, which are not necessarily fixed points, there are very few studies in this field.[23,24]

In this paper, we consider a system in which a stable fixed point coexists with a stable limit cycle. The theoretical analysis of this more complicated case is based on the existence of a generalized (effective) potential with local minima on the corresponding attractors. By using the appropriate analytical technique based on time-scale separation and averaging, an analytical expression for this generalized potential is derived. An interesting aspect of this analysis is that the origin of the generalized potential can be traced back to the injection

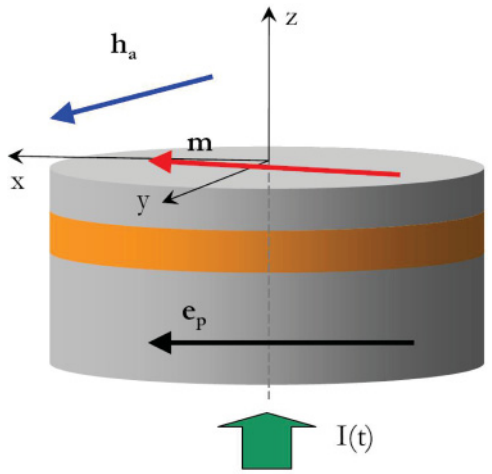

FIG. 1. (Color online) Sketch of a trilayer spin-transfer nano-oscillator.

of electric current in the device, which becomes an open system driven in out-of-equilibrium steady state. By using this generalized potential, we show that the aforementioned stochastic resonance can be studied by using the appropriate nonautonomous stochastic differential equation for the magnetic free energy. The solution of such an equation determines the amplitude of the periodic response of the system at the forcing frequency as a function of temperature and ac current amplitude. The characteristic nonmonotonic dependence on temperature is typical of stochastic resonance. We show that this resonance effect in STNOs occurs both in the classical case of subthreshold ac excitation[20] as well as in the suprathreshold case.[25]

The paper is organized as follows: In Sec. II, the Landau-Lifshitz-Slonczewski (LLS) magnetization dynamics driven by dc and ac injected currents is studied by applying appropriate averaging techniques to the Fokker-Planck equation. This procedure leads to the derivation of a periodically driven stochastic differential equation for the energy. By analytically studying this equation, conditions for the onset of intrawell stochastic resonance involving self-oscillations and equilibria are given. In Sec. III, the proposed approach is used to analyze the intrawell stochastic resonance for a typical STNO. The accuracy of the theoretical predictions is supported by numerical simulations of the LLS dynamics. Finally, in Sec. IV, conclusions and perspectives are outlined.

II. TECHNICAL DISCUSSION

We consider a spin-valve trilayer structure with two ferromagnetic layers, i.e., the free and the fixed layers, separated by a conductive nonmagnetic spacer (see Fig. 1). Both ferromagnetic layers are assumed to be uniformly magnetized. The assumption of spatially uniform magnetization represents a significant simplification of the problem from the mathematical point of view, but has proved to be reasonably effective in the prediction of most aspects of synchronization for STNOs with nanoscale dimensions.[13–19] Moreover, it has been shown[26] that the parametric excitation of spatially inhomogeneous perturbations of magnetization possibly leading to spin-wave instabilities in nanoscale STNOs occurs for high values of applied field and injected currents. The study of this issue is far beyond the scope of this paper and will be addressed in future works.

It is assumed in the sequel that the injected current $I(t)$ is composed of a dc component and a time-harmonic microwave component at given frequency ω (with period $T_\omega = 2\pi/\omega$):

$$I(t) = I_{\rm dc} + I_{\rm ac}\sin(\omega t). \tag{1}$$

It is also assumed that $I_{\rm dc}$ is above the threshold to induce magnetization self-oscillations. Furthermore, the external magnetic field is applied in the film plane, and the orientation of the fixed-layer magnetization is assumed to be constant. Spin-transfer oscillators under these excitation conditions have been extensively studied experimentally.[2]

Magnetization dynamics in the free layer is governed by the Landau-Lifshitz-Slonczewski equation, which can be written in normalized form as follows:

$$\frac{d\mathbf{m}}{dt} = -\mathbf{m}\times(\mathbf{h}_{\rm eff}+\mathbf{h}_{\rm th}) - \alpha\mathbf{m}\times[\mathbf{m}\times(\mathbf{h}_{\rm eff}+\mathbf{h}_{\rm th})] + \beta(t)\frac{\mathbf{m}\times(\mathbf{m}\times\mathbf{e}_p)}{1+c_p\mathbf{m}\cdot\mathbf{e}_p}, \tag{2}$$

where $\mathbf{m}$ is the unit vector in the direction of the free-layer magnetization, $\mathbf{h}_{\rm eff}$ is the effective field normalized by the free-layer saturation magnetization M_s, time is measured in units of $(\gamma M_s)^{-1}$ (γ is the absolute value of the gyromagnetic ratio), and α is the damping constant. The function $\beta(t)$ is proportional to $I(t)$ (positive when electrons flow from the free to the fixed layer) and measures the intensity of the spin-transfer effect, while $\mathbf{e}_p$ is the unit vector in the direction of the fixed-layer magnetization. The relationship between the current $I(t)$ and the normalized one $\beta(t)$ is expressed[3] as $\beta(t) = b_p I(t)/(AJ_p)$, where $b_p = 4P^{3/2}/[3(1+P)^3 - 16P^{3/2}]$, A is the device cross-sectional area, and $J_p = \mu_0 M_s^2 |e| d/\hbar$ is a characteristic current density (μ_0 is the vacuum permeability, e is the electron charge, d is the thickness of the free layer, and $\hbar$ is the reduced Planck constant). The parameter b_p depends on the polarization factor $0 < P < 1$ of the fixed layer.[1] The coefficient $c_p = (1+P)^3/[3(1+P)^3 - 16P^{3/2}]$ in Eq. (2) takes into account the angular dependence of spin-transfer torque.[1] Since $J_p \sim 10^9$ A cm^{-2}, one concludes that, for typical experimental conditions, $\beta(t) \ll 1$. The function $\beta(t)$ is decomposed as follows:

$$\beta(t) = \beta_{\rm dc} + \beta_{\rm ac}\sin(\omega t). \tag{3}$$

The effective field is obtained as the negative gradient of the normalized free-energy density g_L:

$$g_L(\mathbf{m},\mathbf{h}_a) = \tfrac{1}{2}D_x m_x^2 + \tfrac{1}{2}D_y m_y^2 + \tfrac{1}{2}D_z m_z^2 - \mathbf{m}\cdot\mathbf{h}_a, \tag{4}$$

which leads to the following expression:

$$\mathbf{h}_{\rm eff} = -D_x m_x \mathbf{e}_x - D_y m_y \mathbf{e}_y - D_z m_z \mathbf{e}_z + \mathbf{h}_a, \tag{5}$$

where D_x, D_y, D_z are the effective demagnetizing factors taking into account shape and crystalline anisotropy. The presence of thermal fluctuations is taken into account by augmenting the effective field $\mathbf{h}_{\rm eff}$ in Eq. (2) with an isotropic vector Gaussian-white-noise thermal field $\mathbf{h}_{\rm th}$, the variance ν^2 of which is derived from the Einstein relation[27]

(fluctuation-dissipation relation)

$$\nu^2 = \frac{2\alpha}{\mu} = 2\alpha \frac{k_B T}{\mu_0 M_s^2 V}, \tag{6}$$

where T is the temperature, V is the volume of the free layer, and k_B is the Boltzmann constant.

The dynamical system described by Eq. (2), even when thermal fluctuations are neglected, may exhibit very complex behaviors[8] (nonlinear resonance, quasiperiodicity, synchronization, and chaos) since the right-hand side explicitly depends on time due to the microwave component of the current $I(t)$. In the following, by using the formalism based on stochastic processes on graphs,[24,28,29] we derive a theoretical model that allows us to study the synchronization of thermally induced transitions between out-of-equilibrium magnetization regimes with the injected ac current. It will be demonstrated that such synchronization is associated with the occurrence of a novel stochastic resonance effect.

A. Deterministic dynamics

Let us first consider the case when only dc current is injected ($\beta_{\rm dc} \neq 0$, $\beta_{\rm ac} = 0$) and thermal fluctuations are neglected. In this situation, a complete dynamical stability diagram can be obtained by studying the bifurcations of fixed points and limit cycles of the autonomous LLS dynamics.[3] The limit cycles are special periodic oscillations $\mathbf{m}_p(t)$ of period T_p over which the average energy balance is zero:

$$\begin{aligned} &g_L(T_p) - g_L(0) \\ &= -\alpha \int_0^{T_p} \left\{ |\mathbf{m}_p \times \mathbf{h}_{\rm eff}(\mathbf{m}_p)|^2 \right. \\ &\quad \left. - \frac{\beta_{\rm dc}}{\alpha} [\mathbf{m}_p \mathbf{h}_{\rm eff}(\mathbf{m}_p)] \cdot \frac{\mathbf{m}_p \times \mathbf{e}_p}{1 + c_p \mathbf{m}_p \cdot \mathbf{e}_p} \, dt \right\} = 0. \end{aligned} \tag{7}$$

It has been shown[3] that existence, number, and stability of magnetization self-oscillations can be studied by analyzing the zeros of the Melnikov functions $M_k(g,\beta_{\rm dc}/\alpha)$ defined below for the conservative trajectories $\mathbf{m}_k(t,g)$ of period $T_k(g)$, such that $g_L[\mathbf{m}_k(t,g)] = g$ for each central region Ω_k of the energy landscape:

$$\begin{aligned} &M_k(g,\beta_{\rm dc}/\alpha) \\ &= \int_0^{T_k(g)} \left(|\mathbf{m}_k(t,g) \times \mathbf{h}_{\rm eff}[\mathbf{m}_k(t,g)]|^2 - \frac{\beta_{\rm dc}}{\alpha} \{ \mathbf{m}_k(t,g) \right. \\ &\quad \left. \times \mathbf{h}_{\rm eff}[\mathbf{m}_k(t,g)] \} \cdot \frac{\mathbf{m}_k(t,g) \times \mathbf{e}_p}{1 + c_p \mathbf{m}_k(t,g) \cdot \mathbf{e}_p} \right) dt \, . \end{aligned} \tag{8}$$

It is clear that

$$M_k(g,\beta_{\rm dc}/\alpha) = M_k^0(g) + \frac{\beta_{\rm dc}}{\alpha} M_k^1(g). \tag{9}$$

It has been also shown[3] that, for some applied magnetic field, an equilibrium point and a limit cycle may coexist. This coexistence usually occurs for dc current values $\beta_{\rm dc}^- < \beta < \beta_{\rm dc}^+$, where $\beta_{\rm dc}^-$, $\beta_{\rm dc}^+$ are two critical values corresponding to semistable limit-cycle bifurcation and Hopf bifurcation, respectively. It is worthwhile to remark that, for $\beta < \beta_{\rm dc}^-$, there is only a stable equilibrium, whereas, for $\beta > \beta_{\rm dc}^+$, there is only a stable limit cycle.

The outlined Melnikov theory provides a method to predict the energy corresponding to steady magnetization self-oscillations, but gives no information concerning energy relaxations toward these self-oscillations for a given initial condition. Due to the fact that $\alpha \ll 1$ and $\beta_{\rm dc} \ll 1$ (with ratio $\beta_{\rm dc}/\alpha$ of the order of unity), two time scales are present in these magnetization relaxations: a fast one, which corresponds to the precessional motion of magnetization, and a slow one, at which appreciable energy changes occur. This means that the magnetization executes many precessional oscillations during the relaxation process. Besides, over one precessional period, the actual motion is very close to the conservative one. For this reason, the averaging over one precessional period can be used and this leads to the following equation[29] for the energy g:

$$\frac{dg}{dt} = -\alpha \frac{M_k(g,\beta_{\rm dc}/\alpha)}{T_k(g)}. \tag{10}$$

The latter equation can be put in the form

$$\frac{dg}{dt} = -\alpha \frac{\partial U_k}{\partial g} \tag{11}$$

by introducing the effective potential $U_k(g)$:

$$U_k(g) = \int_{g_k^-}^{g} \frac{M_k(u,\beta_{\rm dc}/\alpha)}{T_k(u)} \, du = U_k^0 + \frac{\beta_{\rm dc}}{\alpha} U_k^1(g), \tag{12}$$

where g_k^- is the lower bound of the energy in the central region Ω_k. The dynamics described by Eq. (11) is a relaxation toward minima of the effective potential $U_k(g)$. It is worth to remark that the extrema of $U_k(g)$ include both equilibria and limit cycles.

Let us now introduce a time-harmonic injected current $\beta_{\rm ac} \sin(\omega t)$ such that $\beta_{\rm ac} \ll \beta_{\rm dc}$. We assume that this forcing term changes on a much slower time scale than than the one associated with the precessional dynamics [$T_\omega = 2\pi/\omega \gg T_k(g)$ sufficiently far from the saddles]. In this situation, the same line of reasoning used to justify the averaging of the dynamic equation over one precessional period can be applied, leading to the following equation for the slow dynamics of the energy:

$$\frac{dg}{dt} = -\alpha \frac{\partial U_k}{\partial g} - \beta_{\rm ac} \frac{\partial U_k^1}{\partial g} \sin(\omega t). \tag{13}$$

This is a periodically perturbed version of the relaxation equation (11) that describes the slowly forced energy dynamics far from the saddles.

Next, we show that, in the presence of thermal fluctuations, the energy dynamics can be described in terms of a periodically perturbed stochastic differential equation.

B. Effects of thermal fluctuations

First, let us rewrite Eq. (2) in a more compact form[30] equivalent to Eq. (2):

$$\frac{d\mathbf{m}}{dt} = \mathbf{m} \times \frac{\partial g_L}{\partial \mathbf{m}} + \alpha \mathbf{m} \times \left(\mathbf{m} \times \frac{\partial \Phi}{\partial \mathbf{m}} \right) - \nu \mathbf{m} \times \mathbf{h}_N, \tag{14}$$

where the function $\Phi(\mathbf{m},\mathbf{h}_a,t)$ is given by the formula

$$\Phi(\mathbf{m},\mathbf{h}_a,t) = g_L(\mathbf{m},\mathbf{h}_a) + \frac{\beta(t)}{\alpha} \ln(1 + c_p \mathbf{m} \cdot \mathbf{e}_p)/c_p, \tag{15}$$

and $\mathbf{h}_N(t)$ is the standard isotropic Gaussian-white-noise process such that $\mathbf{h}_{\rm th}(t) = \nu \mathbf{h}_N(t)$. According to the theory of stochastic differential equations,[31] we interpret Eq. (14) in the sense of Stratonovich, which implies that the magnetization vector field describes a stochastic process evolving on the unit sphere $|\mathbf{m}| = 1$. The Fokker-Planck equation associated with Eq. (14) has the form of a continuity equation on the unit sphere

$$\frac{\partial W}{\partial t} = -\nabla_\Sigma \cdot \mathbf{J}, \tag{16}$$

where $W(\mathbf{m},t)$ is the transition probability density function, $\nabla_\Sigma \cdot \mathbf{J}$ is the divergence operator on the unit sphere, while $\mathbf{J}$ is the probability current:

$$\mathbf{J} = (\mathbf{m} \times \nabla_\Sigma g_L - \alpha \nabla_\Sigma \Phi) W - \frac{\nu^2}{2} \nabla_\Sigma W. \tag{17}$$

Since the noise strength is usually a small quantity $\nu \sim \sqrt{\alpha}$ in typical situations, the analysis of magnetization dynamics on a time scale significantly slower than the precessional motion[7,32] can be performed by averaging Eq. (16) with respect to the fast precessional variable. This leads to the following Fokker-Planck equation for the energy g:

$$\frac{\partial \rho_k(g,t)}{\partial t} = -\frac{\partial J_k(g)}{\partial g}, \tag{18}$$

where $\rho_k(g,t)$ is the probability distribution function for the energy such that $W_k(g,t) = \rho_k(g,t)/T_k(g)$, while $J_k(g)$ is the averaged probability current:

$$J_k(g) = -M_k^0(g)\left(\alpha \frac{M_k[g,\beta(t)/\alpha]}{M_k^0(g)} W_k + \frac{\nu^2}{2}\frac{\partial W_k}{\partial g}\right). \tag{19}$$

We observe that the probability current depends explicitly on time through the injected current $\beta(t)$. The equation for $\rho_k(g,t)$ can be transformed in the following form:

$$\frac{\partial \rho_k(g,t)}{\partial t} = \frac{\partial}{\partial g}\left[\left(\alpha \frac{M_k[g,\beta(t)/\alpha]}{T_k} - \frac{\nu^2}{2T_k}\frac{dM_k^0}{dg}\right)\rho_k\right] + \frac{\nu^2}{2}\frac{\partial^2}{\partial g^2}\left(\frac{M_k^0}{T_k}\rho_k\right), \tag{20}$$

where the dependence on g in the right-hand side is tacitly understood. From Eq. (20), the stochastic differential equation (SDE) for the energy can be derived:

$$\frac{dg}{dt} = -\left(\alpha \frac{M_k[g,\beta(t)/\alpha]}{T_k} - \frac{\nu^2}{2T_k}\frac{dM_k^0}{dg}\right) + \nu\sqrt{\frac{M_k^0}{T_k}}\,\mathrm{h}_N(t), \tag{21}$$

where $\mathrm{h}_N(t)$ is the standard one-dimensional (1D) Gaussian white noise. Now, by using the decomposition

$$M_k[g,\beta(t)/\alpha] = M_k^0(g) + \frac{\beta_{\rm dc}}{\alpha} M_k^1(g) + \frac{\beta_{\rm ac}}{\alpha} M_k^1(g)\sin(\omega t), \tag{22}$$

we end up with the following periodically perturbed SDE:

$$\frac{dg}{dt} = -\left[\frac{\alpha M_k^0 + \beta_{\rm dc} M_k^1}{T_k} - \frac{\nu^2}{2T_k}\frac{dM_k^0}{dg}\right] + \nu\sqrt{\frac{M_k^0}{T_k}}\,\mathrm{h}_N(t) - \beta_{\rm ac}\frac{M_k^1}{T_k}\sin(\omega t). \tag{23}$$

It has been shown that in the unperturbed (autonomous $\beta_{\rm ac} = 0$) case, the stationary distribution $W_k^{\rm eq}(g)$ has the expression[7]

$$W_k^{\rm eq}(g) = \frac{1}{Z(\mu)} e^{-\mu V_k(g)}, \tag{24}$$

where the function $V_k(g)$ has the role of an effective potential:

$$V_k(g) = \int_{g_k^-}^{g} \frac{M_k(u)}{M_k^0(u)}\,du + d_k, \tag{25}$$

where d_k is an integration constant to be found by imposing the continuity of $V_k(g)$ across the different central regions Ω_k, while $Z(\mu)$ is a factor that guarantees the normalization condition of the probability distribution function $W(g)$ on the whole state space,[7,29] and μ is defined by formula (6).

It turns out that the effective potential $V_k(g)$ plays the key role in the analysis of stochastic resonance in STNOs for the following reasons:

(i) The effective potential $V_k(g)$ governs the autonomous stochastic dynamics. In fact, according to Eq. (24), the magnetization regimes (equilibria, limit cycles) corresponding to minima of $V_k(g)$ are the most probable in the stochastic dynamics, whereas maxima are the least probable states. We note the analogy between the effective potential $V_k(g)$ and $U_k(g)$, which controls the deterministic energy dynamics.

(ii) $V_k(g)$ determines effective energy barriers between various states of magnetization dynamics. For this reason, it is instrumental for computing the thermal transition rates between magnetization regimes as a function of the injected dc current.

(iii) Stochastic resonance occurs when the appropriate time-scale matching condition is satisfied between these thermal transition rates and the period of a weak external ac excitation. In fact, the mechanism of stochastic resonance is based on "tuning" the periodic deformation of the wells around minima of $V_k(g)$, produced by the weak ac excitation, with the noise-induced hopping between such minima.

C. Intrawell thermal transitions between equilibria and self-oscillations

In the following, we analyze the interesting case of thermally induced transitions between a stable equilibrium g_s and a stable self-oscillation g_a coexisting in the same well of the energy landscape (intrawell transitions) and separated by an unstable limit cycle g_r. Such a coexistence usually occurs for dc current values $\beta_{\rm dc}$ between two critical values $\beta_{\rm dc}^-$, $\beta_{\rm dc}^+$ corresponding to semistable limit-cycle bifurcation and Hopf bifurcation,[3] respectively.

By using the effective potential $V(g)$ (the dependence on the index k is tacitly omitted), the thermal transition rates between g_s and g_a (and vice versa), in the absence of ac current, can be computed. In fact, in the (moderately) low-temperature limit $\mu\Delta V \gg 1$, the effective potential barriers between the equilibrium and the limit cycle and vice versa are such that

$$\mu[V(g_r) - V(g_s)] \gg 1, \quad \mu[V(g_r) - V(g_a)] \gg 1. \tag{26}$$

Under these assumptions, the equilibrium within each potential well will be reached much faster than the equilibrium between different potential wells.[27] For this reason, the distribution

$W(g,t)$ can be approximated as follows around the minima of $V(g)$:

$$W(g,t) = W(g_s,t)e^{-\mu[V(g)-V(g_s)]}, \quad g \in [g_s,g_r'] \tag{27}$$

$$W(g,t) = W(g_a,t)e^{-\mu[V(g)-V(g_a)]}, \quad g \in [g_r'',g_d] \tag{28}$$

where the potential wells around g_s and g_a span the energy ranges $[g_s,g_r']$ and $[g_r'',g_d]$, with g_d being an energy saddle. This implies that the probability density function $W(g,t)$ is strongly peaked around local minima of $V(g)$. Now, in order to study the transient dynamics of energy according to the Kramers' treatment of particle escape from a potential well, it is enough to consider the dynamics of the relative portions $n_a(t)$ and $n_s(t)$ of the distribution around g_a and g_s, respectively, by using the approximations (27) and (28):

$$n_s(t)=W(g_s,t)e^{\mu V(g_s)}Z_s, \quad Z_s=\int_{g_s}^{g_r'} e^{-\mu V(g)}T(g)\,dg, \tag{29}$$

$$n_a(t)=W(g_a,t)e^{\mu V(g_a)}Z_a, \quad Z_a=\int_{g_r''}^{g_d} e^{-\mu V(g)}T(g)\,dg. \tag{30}$$

Despite the fact that $W(g,t)$ is very small in the interval $[g_r',g_r'']$, there is a net flow of probability through this region from the overpopulated to the underpopulated well. By assuming that the probability current is constant in the above interval, namely, $J(g,t) = J(g_r,t)\,, \forall g \in [g_r',g_r'']$ [and, as a consequence, divergence-free $\partial/\partial g J(g,t) = 0\,, \forall g \in [g_r',g_r'']$], we find that, during relaxation toward equilibrium, there will be no appreciable change in the probability density far from local minima g_s and g_a. Therefore, $n_a(t) + n_s(t) = 1$ and any increase in $n_a(t)$ will result in a decrease of $n_s(t)$ (and vice versa). Then, after some algebra, the rate equations for $n_s(t)$ and $n_a(t)$ are obtained from the Fokker-Planck equation (20):

$$\frac{dn_s}{dt} = -\frac{dn_a}{dt} = \frac{\nu^2}{2}\left(\frac{n_a(t)}{Z_a} - \frac{n_s(t)}{Z_s}\right)\frac{1}{S_r} = \frac{n_a(t)}{\tau_{as}} - \frac{n_s(t)}{\tau_{sa}}, \tag{31}$$

where the coefficient S_r is

$$S_r = \int_{g_r'}^{g_r''} \frac{e^{\mu V(g)}}{M^0(g)}\,dg. \tag{32}$$

From Eq. (31), the transition rates $1/\tau_{sa}$ and $1/\tau_{as}$ between the equilibrium g_s and the limit cycle g_a and vice versa can be derived as function of β/α. In fact, by using appropriate Taylor expansions of $V(g)$ around g_s, g_a, and g_r, one can derive approximate expressions for the coefficients Z_s, Z_a, S_r defined by Eqs. (29), (30), and (32). This eventually results in the formulas[28,29]

$$\frac{1}{\tau_{sa}} = \alpha M^0(g_r)\frac{V'(g_s)}{T(g_s)}\sqrt{\frac{\mu|V''(g_r)|}{2\pi}}e^{-\mu[V(g_r)-V(g_s)]}, \tag{33}$$

$$\frac{1}{\tau_{as}} = \frac{\alpha M^0(g_r)}{2\pi T(g_a)}\sqrt{V''(g_a)|V''(g_r)|}e^{-\mu[V(g_r)-V(g_a)]}. \tag{34}$$

It is worthwhile to remark that the transition times τ_{sa},τ_{as} between the equilibrium and the self-oscillation (and vice versa) depend on the curvature of the function $V(g)$ and on the potential barrier. Therefore, they may be very different from each other depending on the injected dc current.

Next, we discuss the forced (nonautonomous) dynamics described by Eq. (23) and the occurrence of intrawell stochastic resonance involving stationary and self-oscillating magnetization regimes.

D. Analysis of intrawell stochastic resonance

Let us now consider the magnetization dynamics induced by the injection of a low-frequency spin-polarized current $\beta_{ac} \neq 0$. We recall that the onset of classical stochastic resonance[20] is referenced to the overdamped motion of a Brownian particle in a symmetric bistable potential, in the presence of noise and periodic forcing, when the following time-scale matching condition holds:

$$2T_K = T_\omega\,, \tag{35}$$

where T_K is the average noise-induced transition time between the minima of the potential and T_ω is the period of the forcing term.

We observe that the nonautonomous SDE (23) has a formal structure analogous to the one described in the classical problem.[20] In fact, the role of the bistable potential is now played by the effective potential $V(g)$. Despite this formal similarity between the governing equations, the problem under consideration is more general for at least two reasons:

(1) The minima of $V(g)$ separated by an effective potential barrier ΔV may represent either equilibria or self-oscillations.[7] This means that $V(g)$ represents an out-of-equilibrium potential. We remark that the developed approach is not limited to the analysis of intrawell magnetization motion, but can be applied to study the transitions between magnetization regimes located also in different regions of the energy landscape. However, the transitions between a stable equilibrium and a stable limit cycle coexisting in the same potential well (intrawell transitions) are of special interest.

(2) In the classical problem, the bistable potential is symmetric. This implies that the thermal transitions between the local equilibria occur with the same rate $r_K = 1/T_K$. On the contrary, in the case of magnetization dynamics (in the limit of high potential barrier $\mu\Delta V \gg 1$), the transition times τ_{sa},τ_{as} depend on the curvature of the function $V(g)$ as well as on the potential barrier. Therefore, the rates corresponding to the transition from the equilibrium to the limit cycle and vice versa may be very different. In addition, in the case of asymmetry of the potential, the "golden rule" of time-scale matching $2T_K = T_\omega$ is not applicable. In fact, quoting[20] Gammaitoni *et al.*, "...there exists no obvious time-scale matching condition in asymmetric systems." For this reason, in order to look for conditions in which the transitions are synchronized with the external ac current, we need first to find conditions when, in the absence of ac current, the transition rates between the equilibrium and the limit cycle are almost the same.

As far as the period T_ω of the external ac current is concerned, its value satisfies the following time-scale matching condition:

$$\tau_{as} + \tau_{sa} = T_\omega\,. \tag{36}$$

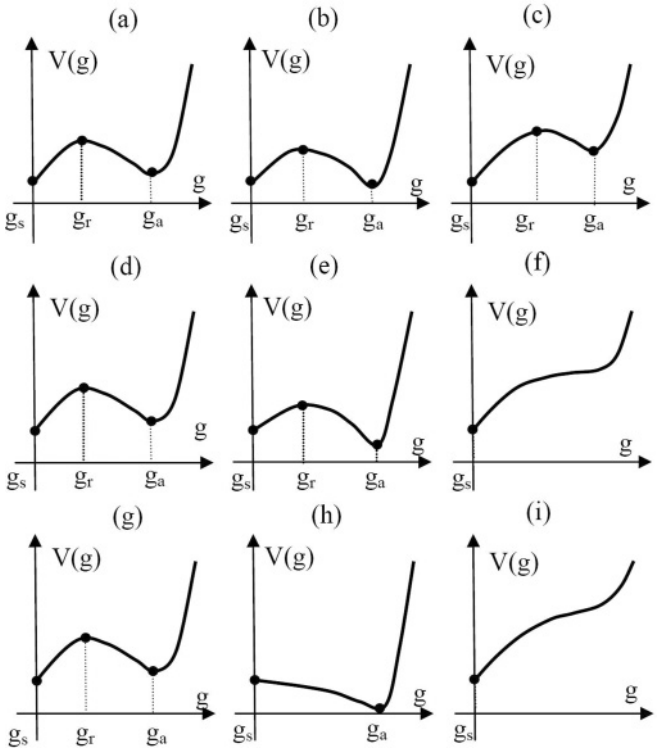

FIG. 2. Effective potential $V(g)$ as function of time in the case of subthreshold (a)–(c), intermediate threshold (d)–(f), and suprathreshold ac current amplitude (g)–(i). The solid lines in the left, middle, and right columns represent a sketch of the effective potential $V(g)$ when the ac current is zero, maximum, and minimum, respectively.

The condition (36) mimics the time-scale matching rule $2T_K = T_\omega$ in the classical stochastic resonance treatment.

It is also worth noting that different situations occur depending on the ac current amplitude $\beta_{\rm ac}$. In fact, in order that both the equilibrium and the self-oscillations remain stable at any time instants, i.e., the effective potential has two local minima for all $\beta(t)/\alpha$, the amplitude $\beta_{\rm ac}$ can not be arbitrary, but must fulfill the constraints

$$\beta_{\rm dc}^- < \beta_{\rm dc} \pm \beta_{\rm ac} < \beta_{\rm dc}^+, \tag{37}$$

which determine two threshold values $\beta_{\rm ac}^\pm$ for $\beta_{\rm ac}$:

$$\beta_{\rm dc}^- < \beta_{\rm dc} - \beta_{\rm ac} \Rightarrow \beta_{\rm ac} < \beta_{\rm ac}^- = \beta_{\rm dc} - \beta_{\rm dc}^-, \tag{38}$$

$$\beta_{\rm dc} + \beta_{\rm ac} < \beta_{\rm dc}^+ \Rightarrow \beta_{\rm ac} < \beta_{\rm ac}^+ = \beta_{\rm dc}^+ - \beta_{\rm dc}. \tag{39}$$

It is convenient to distinguish three cases:

(1) When $\beta_{\rm ac} < \min[\beta_{\rm ac}^-,\beta_{\rm ac}^+]$ (subthreshold case), the effective potential $V(g)$, which depends on time through $\beta(t)/\alpha$, has always two local minima associated with two stable magnetization regimes [see Figs. 2(a)–2(c)].

(2) When $\beta_{\rm ac}^- < \beta_{\rm ac} < \beta_{\rm ac}^+$ (intermediate case), there are certain time intervals where only the stable equilibrium [local minimum of $V(g)$ corresponding to $g = g_s$] exists [see Figs. 2(d)–2(f)].

(3) When $\beta_{\rm ac} > \max[\beta_{\rm ac}^-,\beta_{\rm ac}^+]$ (suprathreshold case), there are certain time intervals where the system admits exclusively either the equilibrium ($g = g_s$) or the self-oscillation regime ($g = g_a$) [see Figs. 2(g)–2(i)].

The periodic response of the system is qualitatively different in these three cases.

III. NUMERICAL RESULTS AND DISCUSSION

In order to check the validity of the proposed theoretical approach, we consider a typical STNO with the following parameters: the effective demagnetizing factors are $D_x = -0.034$, $D_y = 0$, $D_z = 0.68$, the damping is $\alpha = 0.02$, the polarizer is $\mathbf{e}_p = \mathbf{e}_x$, and the applied field is $\mathbf{h}_a = \mathrm{h}_{ax}\mathbf{e}_x$. The saturation magnetization is $\mu_0 \mathrm{M}_s = 1.76$ T, which implies that frequency is measured in units of $\gamma \mathrm{M}_s \approx 310$ GHz and time in units of $(\gamma \mathrm{M}_s)^{-1} \approx 3.2$ ps. The free-layer volume is $V = 1.867 \times 10^{-24}$ m. For an elliptic cross section $A = \pi ab$ with a,b being the long and short semiaxis, respectively, one has $V = \pi abd$ (d is the thickness of the free layer), which yields $2a \approx 72$ nm, $2b \approx 40$ nm, $d \approx 1$ nm. At room temperature $T = 300$ K, the noise amplitude is $\nu = 6 \times 10^{-3}$.

First, we analyze the case when only a dc current is injected in the STNO. By using the Melnikov function (8), one can find that for $\mathrm{h}_{ax} = 0.08$ there are a stable equilibrium $g_s = -0.097$ and a stable self-oscillation g_a, separated by an unstable limit cycle g_r in the range of currents $\beta_{\rm dc}/\alpha \in (0.61,0.7)$. The lower bound $\beta_{\rm dc}^- = 0.61\alpha$ is related to a semistable limit-cycle bifurcation, whereas the upper bound $\beta_{\rm dc}^+ = 0.7\alpha$ is associated with a Hopf bifurcation.[29]

As pointed out before, we first look for injected dc currents that produce the same thermal transition rates in the absence of ac excitation.

To this end, the transition rates $1/\tau_{sa}$ and $1/\tau_{as}$ between the equilibrium g_s and the limit cycle g_a and vice versa have been computed as a function of $\beta_{\rm dc}/\alpha$ according to the formulas (33) and (34). The results of the computation are reported in Fig. 3. We observe that the transition times τ_{as} and τ_{sa} are the same $\sim 5 \times 10^4$ for the injected current value $\beta_{\rm dc} \approx 0.63\alpha$.

In our study, we chose the value $\beta_{\rm dc} = 0.635\alpha$, which produces some asymmetry in the transition times since $\tau_{as} \approx 7 \times 10^4$ and $\tau_{sa} \approx 3 \times 10^4$. This is done on purpose to investigate whether such asymmetry affects the occurrence of stochastic resonance. As one can see from Fig. 3, the effective potential barriers associated with this current value are $\mu\Delta V_{as} \approx 2$ and $\mu\Delta V_{sa} \approx 3.5$. We note that for $\beta_{\rm dc}/\alpha = 0.635$, one has $g_a = 0.039$, $g_r = -0.032$.

We have numerically integrated (with the methods described in the Appendix) the SDE (23) for $\beta_{\rm ac} = 0$ and $\beta_{\rm dc} = 0.635\alpha$. In Fig. 4, the stationary distribution $W_k^{\rm eq}(g)$ computed by using formula (24) is reported along with the normalized occupation histogram obtained from the numerical integration of Eq. (23). The two independent computations are in very good agreement and demonstrate that the chosen time step $\Delta t = 0.1$ is small enough to guarantee sufficient accuracy for the solution of Eq. (23). One can clearly see that the distribution is peaked around the stable equilibrium corresponding to $g_s = -0.097$ and the stable self-oscillation at $g_a = 0.039$, whereas it has a minimum corresponding to the unstable limit cycle $g_r = -0.032$. For chosen values of

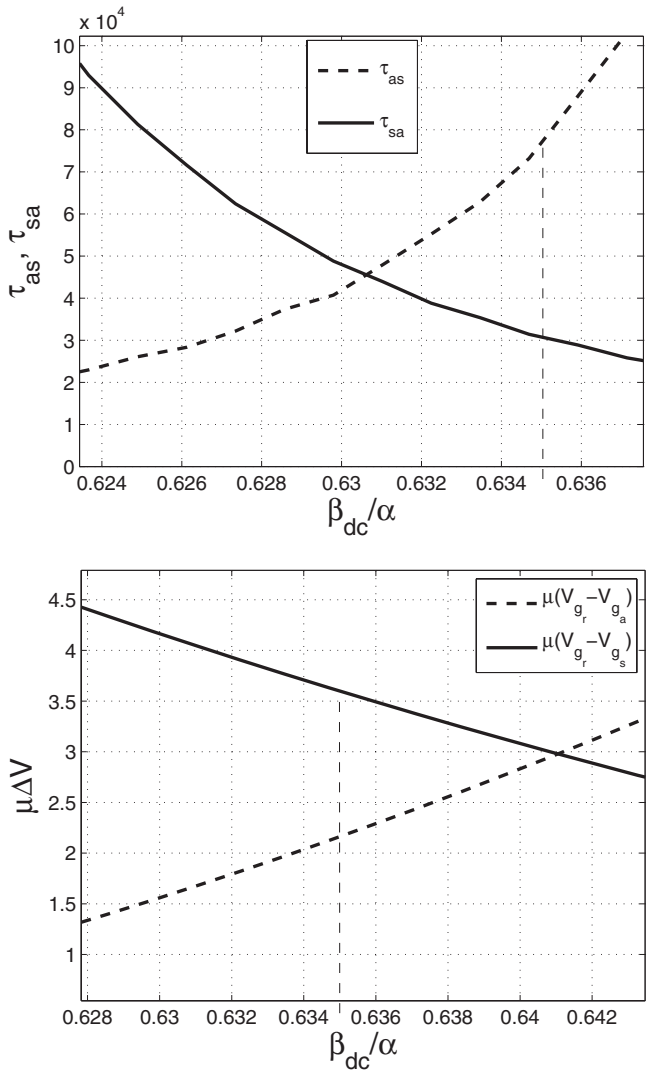

FIG. 3. (a) Transition times τ_{as}, τ_{sa} (dashed, solid lines) as function of β_{dc}/α. (b) Effective potential barrier $\mu\Delta V$ as function of β_{dc}/α. The values of parameters are $\alpha = 0.02$, $D_x = -0.034$, $D_y = 0$, $D_z = 0.68$, $h_{ax} = 0.08$, $\nu = 6 \times 10^{-3}$. In the computations, $T = 300$ K, which yields $\mu \approx 1111$. Vertical dashed lines indicate the value $\beta_{dc}/\alpha = 0.635$ used in the computations.

the parameters, one has $\beta_{ac}^{-} = 0.025\alpha \approx \beta_{dc}/26$ and $\beta_{ac}^{-} = 0.065\alpha \approx \beta_{dc}/10$.

As far as the period of the ac current, we chose $T_\omega = 10^5$ (corresponding to a frequency $f = 3.1$ MHz in physical units), which satisfies the time-scale matching condition (36).

In Fig. 5, the effective potential $V(g)$ is plotted at different times for a subthreshold ac current amplitude. As one can clearly see, the potential wells for the stable magnetization regimes change up and down in time. These variations can be utilized to match the time scale of thermal transition times and eventually obtain a synchronized transition resulting in a strong response of the system at the driving frequency $f = 1/T_\omega$.

In Fig. 6, two realizations of the energy dynamics computed through the numerical integration of Eq. (23) for $\beta_{ac} = 0$ and $\beta_{ac} = \beta_{dc}/35$ are reported. It is apparent that, in the former case, the system exhibits random transitions between

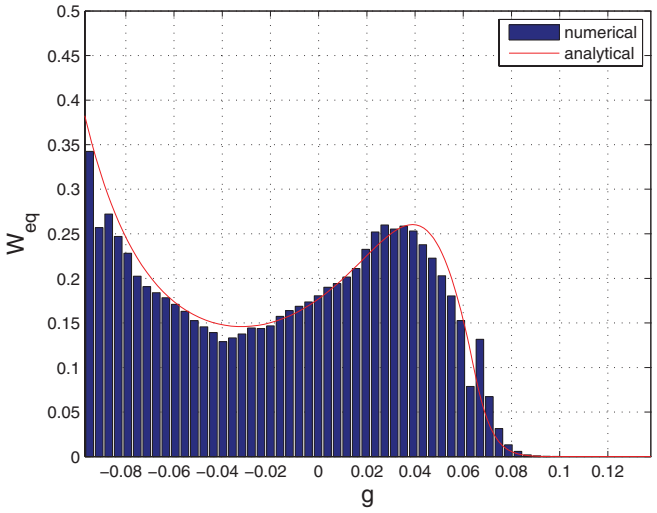

FIG. 4. (Color online) Stationary distribution in the unperturbed case $\beta_{ac} = 0$ and $\beta_{dc} = 0.635\alpha$, $\alpha = 0.02$ (the other parameters are the same as Fig. 3). Solid line is obtained by the analytical expression (24), the normalized occupation histogram has been computed by direct integration of the SDE (23) with a time step $\Delta t = 0.1$.

$g_s = -0.097$ and $g_a = 0.039$, whereas, in the latter case, the noise-induced transitions follow the time behavior of the ac current. This means that synchronization has been realized. In order to study the dependence of the synchronization on the temperature, i.e., the noise amplitude ν, we have performed the following computation:

(i) Equation (23) has been integrated for a time $T_s = 5 \times 10^5$ to find $N = 50$ realizations $g_i(t)$ of the stochastic process $g(t)$.

(ii) The so-called periodogram $P_i(f) = |S_i(f)|^2$ [squared modulus of the fast Fourier transform $S_i(f)$] has been computed for each realization $g_i(t)$.

(iii) The power spectral density of the process $g(t)$ has been estimated by averaging the periodograms (this technique is often referred to as Bartlett's method[33]):

$$S_g(f) = \frac{1}{N} \sum_{i}^{N} P_i(f). \tag{40}$$

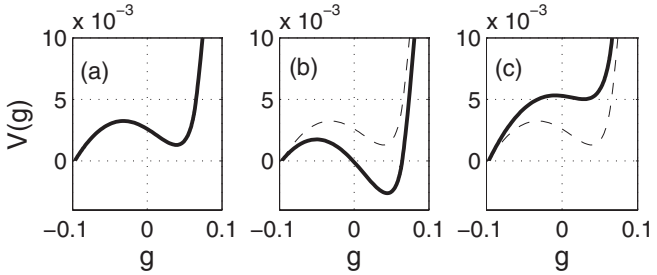

FIG. 5. Effective potential $V_k(g)$ in the case of subthreshold ac current amplitude. The parameters are $\beta_{dc}/\alpha = 0.635$, $\beta_{ac} = \beta_{dc}/35$ (the other parameters are the same as Fig. 3). Solid lines represent the effective potential $V_k(g)$ computed when the ac current is (a) zero, (b) maximum, and (c) minimum. Dashed lines refer to the case $\beta_{ac} = 0$.

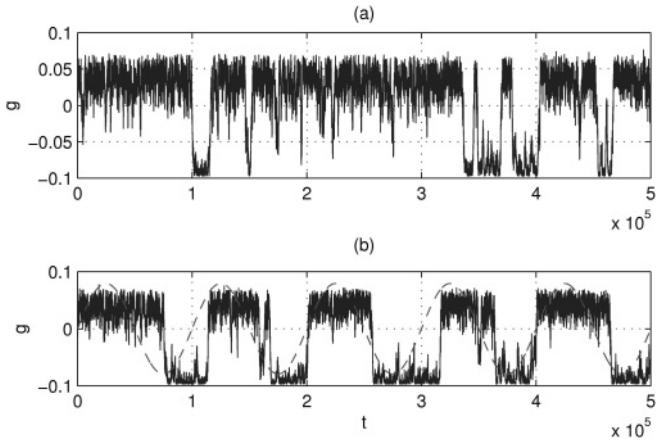

FIG. 6. Time evolution of $g(t)$ when (a) $\beta_{ac} = 0$ and (b) $\beta_{ac} = \beta_{dc}/35$. The dashed line is a guide for the eye, representing a magnified sine waveform associated with the ac current. The other parameters are the same as Fig. 3.

(iv) The value $S_g(f = 1/T_\omega)$ has been extracted.

The results of this procedure are reported in Fig. 7. It is very interesting to observe the qualitative character of the response as a function of the ac current amplitude.

It can be clearly seen that, in the subthreshold case $\beta_{ac} < \beta_{ac}^-$, the amplitude of the periodic response at driving frequency exhibits the nonmonotonic dependence on temperature (noise amplitude ν) typical of stochastic resonance. The computations have been performed for several values of the ac injected current, even two orders of magnitude smaller than the dc component β_{dc}, and the above effect is quite evident.

It is also apparent in Fig. 7 that, for ac current amplitudes slightly above the threshold $\beta_{ac}^- < \beta_{ac} < \beta_{ac}^+$, the monotonic behavior of the periodic response persists, but becomes less and less pronounced as the ac current strength increases. In complete contrast to classical (subthreshold) stochastic resonance, this suprathreshold effect is most pronounced when the deterministic threshold crossings are maximized.[25] This

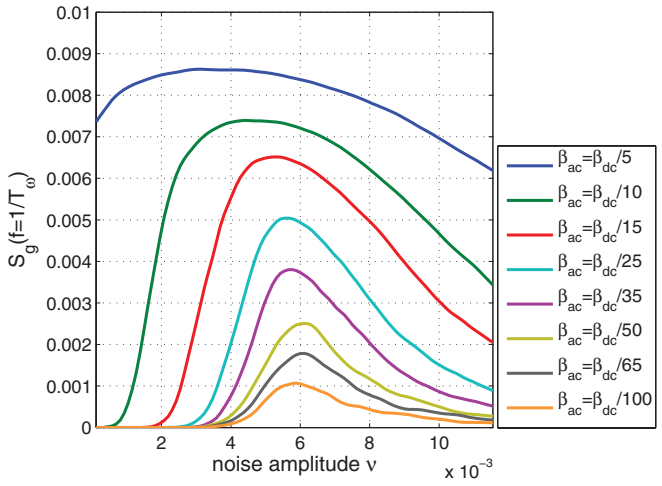

FIG. 7. (Color online) $S_g(f = 1/T_\omega)$ as a function of thermal noise intensity ν and ac current amplitude β_{ac}. The other parameters are the same as Fig. 3.

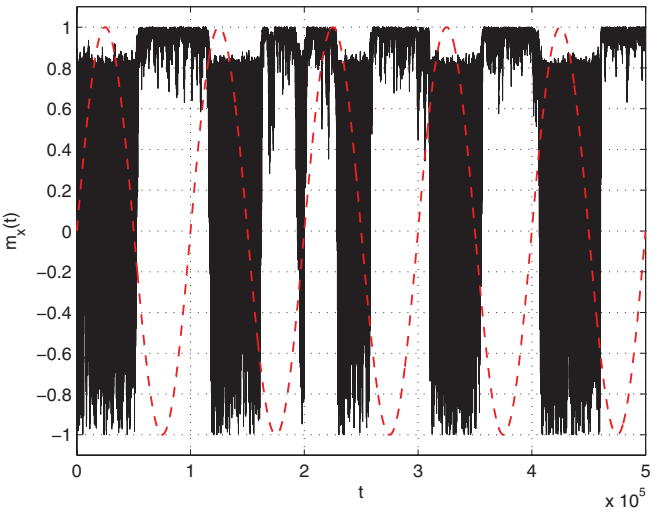

FIG. 8. (Color online) Numerical simulation of the LLS equation (2). The time behavior of m_x shows thermal transitions between magnetization self-oscillation and equilibrium synchronized with a low-frequency weak ac current. The dashed line is a guide for the eye, representing the sine waveform of the ac current. The values of parameters are the same as Fig. 6.

happens for β_{ac} close and beyond the second threshold β_{ac}^+. We also observe that, for increasing ac current amplitudes, the stochastic resonance peak shifts toward smaller noise intensities, meaning that the stronger response is mainly driven by the deterministic dynamics.

Finally, the theoretical predictions discussed above have been compared with full-scale Landau-Lifshitz-Slonczewski simulations[34] for the values of parameters corresponding to the peak of the response $\nu = 6 \times 10^{-3}$ and $\beta_{ac} = \beta_{dc}/35$. The results are reported in Fig. 8, showing excellent agreement with the theory. In fact, one can clearly see that the onset of stochastic resonance produces a sharp synchronization of transitions between a self-oscillating and a stationary magnetization regime.

IV. CONCLUSIONS

The thermally induced synchronization of transitions between magnetization regimes has been analyzed for spin-transfer oscillators. It has been shown that, for appropriate (weak) ac injected current and thermal noise amplitude, the system presents an enhanced periodic magnetization response at the frequency of the ac current. A theoretical approach, based on the separation of time scales in magnetization dynamics, has been developed to investigate these phenomena. By using appropriate averaging techniques, a periodically perturbed stochastic differential equation for the "slow" energy variable has been derived. This approach has been used to analyze thermal transitions between equilibria and self-oscillations located within the same potential well of the energy landscape (intrawell transitions).

It has been shown that the enhanced response is originated by the matching between thermal transition rates between different magnetization regimes (equilibria and self-oscillations),

determined in the absence of ac current, and the frequency of the external ac current. In this respect, it has been demonstrated that the amplitude of the periodic response of the stochastic energy dynamics at the driving frequency exhibits a nonmonotonic behavior with respect to the thermal noise strength (temperature), which is the signature of a general stochastic resonance involving out-of-equilibrium regimes. This stochastic resonance effect occurs both in the subthreshold and in the suprathreshold regimes. The theory is able to accurately predict the conditions for such resonant behavior, as confirmed by the full-scale simulations of the Landau-Lifshitz-Slonczewski dynamics. We expect that the proposed approach can be instrumental for the analysis of experiments on thermally induced synchronization of spin-transfer nano-oscillators. It is believed that the analysis presented in this paper is very general in nature and may be applied to physical problems when steady-state periodic solutions are driven out of equilibrium by interactions with the environment.

APPENDIX: NUMERICAL INTEGRATION OF THE STOCHASTIC ENERGY DYNAMICS

The SDE (23) can be conveniently rewritten in the standard form[31]

$$dg = a(g,t)\,dt + b(g)\,dW, \tag{A1}$$

where the functions $a(g,t)$ and $b(g)$ are

$$a(g,t) = -\frac{\alpha M_k^0 + \beta_{\rm dc} M_k^1}{T_k} + \frac{\nu^2}{2T_k}\frac{dM_k^0}{dg} - \beta_{\rm ac}\frac{M_k^1}{T_k}\sin(\omega t), \tag{A2}$$

$$b(g) = \nu\sqrt{\frac{M_k^0}{T_k}}, \tag{A3}$$

and $W(t)$ is the standard 1D Wiener process. Equation (A1) can be solved by using a Langevin dynamics approach. Namely, the statistical properties of the stochastic process $g(t)$ are determined by computing a sufficiently large number of realizations from the numerical integration of Eq. (A1).

The numerical integration is based on the following explicit derivative-free Milstein time-stepping scheme,[31] which converges strongly with order 1 (and weakly with order 1) to the solution of the Ito SDE:

$$g_{n+1} = g_n + a_n + b_n\Delta W_n + \frac{1}{2\sqrt{\Delta t}}[(\tilde{b}_n - b_n)][(\Delta W_n)^2 - \Delta t], \tag{A4}$$

$$\tilde{b}_n = g_n + a_n + b_n\sqrt{\Delta t}, \tag{A5}$$

$$\Delta W_n = W_{n+1} - W_n \sim N(0,\Delta t), \tag{A6}$$

where $g_n = g(t_n)$, $a_n = a(g_n,t_n)$, $b_n = b(g_n)$, and $W_n = W(t_n)$.

[1] J. C. Slonczewski, J. Magn. Magn. Mater. **159**, L1 (1996).
[2] S. I. Kiselev, J. C. Sankey, I. N. Krivorotov, N. C. Emley, R. J. Schoelkopf, R. A. Buhrman, and D. C. Ralph, Nature (London) **425**, 380 (2003).
[3] G. Bertotti, C. Serpico, I. D. Mayergoyz, A. Magni, M. d'Aquino, and R. Bonin, Phys. Rev. Lett. **94**, 127206 (2005).
[4] S. Urazhdin, N. O. Birge, W. P. Pratt, and J. Bass, Phys. Rev. Lett. **91**, 146803 (2003).
[5] A. Fabian, C. Terrier, S. S. Guisan, X. Hoffer, M. Dubey, L. Gravier, J. P. Ansermet, and J. E. Wegrowe, Phys. Rev. Lett. **91**, 257209 (2003).
[6] I. N. Krivorotov, N. C. Emley, A. G. F. Garcia, J. C. Sankey, S. I. Kiselev, D. C. Ralph, and R. A. Buhrman, Phys. Rev. Lett. **93**, 166603 (2004).
[7] R. Bonin, C. Serpico, G. Bertotti, I. D. Mayergoyz, and M. d'Aquino, Eur. Phys. J. B **59**, 435445 (2007).
[8] Z. Li, Y. C. Li, and S. Zhang, Phys. Rev. B **74**, 054417 (2006).
[9] S. Kaka, M. R. Pufall, W. H. Rippard, T. J. Silva, S. E. Russek, and J. A. Katine, Nature (London) **437**, 389 (2005).
[10] F. B. Mancoff, N. D. Rizzo, B. N. Engel, and S. Tehrani, Nature (London) **437**, 393 (2005).
[11] W. H. Rippard, M. R. Pufall, S. Kaka, T. J. Silva, S. E. Russek, and J. A. Katine, Phys. Rev. Lett. **95**, 067203 (2005).
[12] B. Georges, J. Grollier, M. Darques, V. Cros, C. Deranlot, B. Marcilhac, G. Faini, and A. Fert, Phys. Rev. Lett. **101**, 017201 (2008).
[13] R. Bonin, G. Bertotti, C. Serpico, I. D. Mayergoyz, and M. d'Aquino, Eur. Phys. J. B **68**, 221 (2009).
[14] A. N. Slavin and V. Tiberkevich, IEEE Trans. Magn. **45**, 1875 (2009).
[15] C. Serpico, R. Bonin, G. Bertotti, M. d'Aquino, and I. D. Mayergoyz, IEEE Trans. Magn. **45**, 3441 (2009).
[16] S. Urazhdin, P. Tabor, V. Tiberkevich, and A. Slavin, Phys. Rev. Lett. **105**, 104101 (2010).
[17] M. d'Aquino, C. Serpico, R. Bonin, G. Bertotti, and I. D. Mayergoyz, Phys. Rev. B **82**, 064415 (2010).
[18] M. Quinsat, J. F. Sierra, I. Firastrau, V. Tiberkevich, A. Slavin, D. Gusakova, L. D. Buda-Prejbeanu, M. Zarudniev, J.-P. Michel1, U. Ebels, B. Dieny, M.-C. Cyrille, J. A. Katine, D. Mauri, and A. Zeltser, Appl. Phys. Lett. **98**, 182503 (2011).
[19] M. d'Aquino, C. Serpico, R. Bonin, G. Bertotti, and I. D. Mayergoyz, J. Appl. Phys. **109**, 07C914, (2011).
[20] L. Gammaitoni, P. Hanggi, P. Jung, and F. Marchesoni, Rev. Mod. Phys. **70**, 223 (1998).
[21] X. Cheng, C. T. Boone, J. Zhu, and I. N. Krivorotov, Phys. Rev. Lett. **105**, 047202 (2010).
[22] G. Finocchio, I. N. Krivorotov, X. Cheng, L. Torres, and B. Azzerboni, Phys. Rev. B **83**, 134402 (2011).
[23] M. I. Dykman, D. G. Luchinsky, R. Mannella, P. V. E. McClintock, N. D. Stein, and N. G. Stocks, Pis'ma Zh. Eksp. Teor. Fiz. **58**, 145 (1993).
[24] M. Freidlin, Phys. B (Amsterdam) **306**, 10 (2001).
[25] N. G. Stocks, Phys. Rev. Lett. **84**, 2310 (2000).
[26] G. Bertotti, R. Bonin, M. d'Aquino, C. Serpico, and I. D. Mayergoyz, IEEE Magn. Lett. **1**, 3000104 (2010).

[27]W. F. Brown, Phys. Rev. **130**, 1677 (1963).
[28]C. Serpico, G. Bertotti, I. D. Mayergoyz, M. d'Aquino, and R. Bonin, J. Appl. Phys. **99**, 08G505 (2006).
[29]G. Bertotti, I. D. Mayergoyz, and C. Serpico, *Nonlinear Magnetization Dynamics in Nanosystems* (Elsevier, Amsterdam, 2009).
[30]G. Bertotti, C. Serpico, I. D. Mayergoyz, R. Bonin, and M. d'Aquino, J. Magn. Magn. Mater. **316**, 285 (2007).
[31]P. E. Kloeden, E. Platen, and H. Schurz, *Numerical Solution of SDE Through Computer Experiments* (Springer, Berlin, 1994).
[32]D. M. Apalkov and P. B. Visscher, Phys. Rev. B **72**, 180405 (2005).
[33]A. Papoulis, *Probability, Random Variables, and Stochastic Processes*, 3rd ed. (McGraw-Hill, New York, 1991).
[34]M. d'Aquino, C. Serpico, G. Coppola, I. D. Mayergoyz, and G. Bertotti, J. Appl. Phys. **99**, 08B905 (2006).